imaginary numbers $i\epsilon$ disappear in all propagators and we are only left with a product of i's in front of the integral. From the general structure of diagrams contributing to $G(p)$, one finds that the total number of i's coming from the propagators, the vertices, and the Wick rotation is always even. Hence, below the threshold

$$G^{(*)}(p)=G(p)\,, \tag{B14}$$

and Eq. (B11) follows.

In the proof of Eq. (B12) we follow the same line of reasoning. We use Eqs. (43a), (B7), and (B8) to find

$$\overline{\delta N(p)} = \left[ie^2\int(dk)\,\delta\tilde{g}_\nu(k)\Gamma^\nu(p;p-k;k)G(p-k)\right]^{(*)}. \tag{B15}$$

Then we change the integration variable $k\to -k$ and use the property that $\delta\tilde{g}_\nu(k)$ is an odd function of k. Finally, we employ the argument involving the Wick rotation to show that the expression in the bracket in (B15) does not change under (*) conjugation below the threshold. On account of (43b), this gives the desired relation (B12).

PHYSICAL REVIEW D VOLUME 2, NUMBER 12 15 DECEMBER 1970

Field-Theory Realization of the Droplet Model*

Shau-Jin Chang

Physics Department, University of Illinois, Urbana, Illinois 61801†
and
Stanford Linear Accelerator Center, Stanford University, Stanford, California 94305

(Received 10 August 1970)

We demonstrate with two field-theoretic models that the operator droplet model proposed by Chou and Yang can be understood as due to the contribution from a class of leading Feynman diagrams at $s=\infty$. In the first model, we consider a theory which consists of both a strong and an electromagnetic interaction. The purpose of introducing two types of interactions is to supply a natural division between the production of particles and the interaction between the jets. In this model, the sum of pure photon-exchange diagrams leads automatically to an expression identical to that of the operator droplet model. Limitations and generalizations of the model are investigated. The second model is derived from pure quantum electrodynamics. We find that an operator-droplet-model formulation can reproduce leading amplitudes in quantum electrodynamics, including those which give rise to $(\ln s)^N$ behavior. This confirms and generalizes an earlier result of Lee. We demonstrate explicitly how the N-bubble diagrams should be treated in this calculation. By including diagrams related to one another by covariance, a reference-frame-independent result always emerges. These frame-independent results coincide with earlier calculations based on the usual Feynman rules.

I. INTRODUCTION

A DROPLET model has been proposed by Chou, Yang,[1] and their co-workers in order to understand qualitatively high-energy scattering. In particular, they conjectured that hadron production processes can be understood through an operator version of the droplet model. In a recent article,[2] the operator droplet model was put into an elegant and useful form by Lee. Lee then applied the operator droplet model to quantum electrodynamics (QED), with the identification of the matter density ρ and the charge density. He demonstrated that this model can reproduce the field-theoretic results of Cheng and Wu[3] as to impact factors. It is interesting to know whether or how more complicated $(\ln s)^N$-dependent terms can be obtained in Lee's formulation. It is also important to find out if his conclusion can be generalized to high-order processes.

The purpose of this paper is to show that the operator-droplet-model results can indeed be obtained by summing a proper set of diagrams. By establishing the connection between a physical model and a category of Feynman diagrams, one can hope to gain some insights and understanding of the model, such as its possible limitations and generalizations. This is one of the important reasons for carrying out a systematical analysis of Feynman diagrams.

The first model that we shall study is a combination of a pseudoscalar-meson theory and the electromagnetic (EM) interaction. We first analyze a diagram by

* Work supported in part by the U. S. Atomic Energy Commission and the National Science Foundation under Contract No. NSF GP 19433.

† Permanent address.

[1] T. T. Chou and C. N. Yang, Phys. Rev. **170**, 1591 (1968); **175**, 1832 (1968); J. Benecke, T. T. Chou, C. N. Yang, and E. Yen, *ibid.* **188**, 2159 (1969).

[2] B. Lee, Phys. Rev. D 1, 2361 (1970).

[3] H. Cheng and T. T. Wu, Phys. Rev. Letters 22, 666 (1969); Phys. Rev. **182**, 1852 (1969); **182**, 1868 (1969); **182**, 1873 (1969); **182**, 1899 (1969).

decomposing it into units which are joined together by pure photon exchange.[4] Each of these units defines a primitive piece, as introduced in Paper III. For simplicity, we shall ignore further EM interactions within these primitive units (hereafter referred to as hadronic blobs). In this way, we make a division between the hadronic interactions within the blobs and the EM interactions between the blobs. The dynamical distinction of these two interactions is important in the first model in order to achieve our conclusion. An especially simple set of diagrams according to this classification is shown in Fig. 1, in which there are no further hadronic bubbles lying between the blobs associated with the incident particles. By summing over diagrams of this category, we obtain a result which can be identified with that of an operator droplet model with an s-independent potential. This potential is the two-dimensional Fourier transform of the one-photon propagator. Contributions due to further photon-photon interactions can be partially handled if one modifies the potential to include all connected diagrams. The modified potential acquires an s dependence.

In pure QED calculations, the sum of diagrams in Fig. 1 no longer exponentiates to a droplet-model form. However, the operator droplet model can be recovered formally if one includes *all* leading graphs and if proper care is taken in defining the infinite-momentum matrix element of the product of currents. A formal perturbative calculation reveals that for a certain important class of final and intermediate states, the matrix element of the currents diverges logarithmically at large s. This indicates that there is some implicit s dependence in the QED expression described by the operator droplet model. This implicit s dependence is associated with the increase of the available $\ln p_+$ phase space at $s \to \infty$.[5] Once we realize the origin of this hidden $\ln s$ dependence, we can reproduce all the leading amplitudes in QED from an operator-droplet-model expression suggested by Chou and Yang[1] and by Lee.[2]

The paper is organized as follows. In Sec. II, we consider a model in which a strong interaction and the EM interaction are treated separately. We analyze a particular category of diagrams due to multiphoton exchange and show that it leads naturally to an expression identical to the operator droplet model. A simpler and more straightforward derivation is obtained in Sec. III, based on essentially the same assumptions. In Sec. IV, a generalization of this model to include a larger set of diagrams is outlined. In Sec. V, we demonstrate how the operator droplet model can be used to compute the leading QED diagrams, including those which give rise to $(\ln s)^N$ behavior at large s. The conclusion and a comparison of our model to Feynman's parton model[6,7] comprise the contents of the last section. We also include a short appendix to demonstrate how one can obtain commutator relations on the light cone from the conventional equal-time commutator relations.

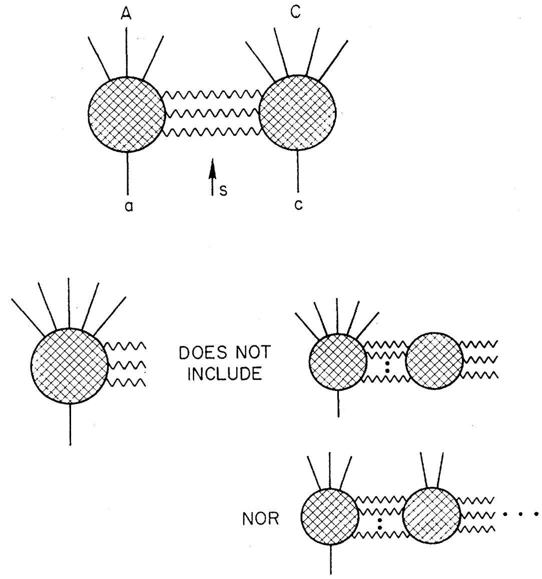

FIG. 1. Pure multiphoton-exchange diagram without further photon-photon interactions. In Secs. II and III the blobs contain only the strong interactions.

II. MULTIPHOTON-EXCHANGE DIAGRAMS

We consider a simple field-theory model with both a strong and an EM interaction, $\mathcal{L}_{\rm int} = \mathcal{L}_s + \mathcal{L}_{\rm EM}$. We may take the strong interaction, for example, as pseudoscalar mesons ϕ coupled to nucleons ψ through the coupling $\mathcal{L}_s = ig\bar{\psi}i\gamma_5(\boldsymbol{\tau}/2)\psi\phi$, or as quark-quark interactions. The conclusions of this paper do not depend on the detailed structure of the strong interaction as long as there is no *fundamental* strongly interacting vector field. The EM interaction, on the other hand, is mediated by a vector field (the Maxwell field) $\mathcal{L}_{\rm EM} = e j_\mu A^\mu$, with

$$j_\mu = \bar{\psi}\gamma_\mu\psi\,. \qquad (2.1)$$

To avoid infrared divergences, we give our photon a fictitious mass μ. Note that our results are readily applicable to pure hadronic processes if one replaces the photon by a vector meson, or a flat Pomeranchukon. We call our vector meson a "photon" solely for simplicity.

In Paper II, we demonstrated that those diagrams whose contribution remains large at large s but fixed t

[4] S. J. Chang and S. Ma, Phys. Rev. **180**, 1506 (1969); **188**, 2385 (1969), hereafter referred to as I and II; S. J. Chang and P. M. Fishbane, Phys. Rev. D **2**, 1104 (1970), hereafter referred to as III.

[5] See Sec. III in III.

[6] R. P. Feynman, in *Proceedings of the Third International Conference on High-Energy Collisions, SUNY, Stony Brook, N. Y., 1961* (Gordon and Breach, New York, 1969).

[7] J. D. Bjorken, invited paper at the APS New York meeting, 1969 (unpublished); J. D. Bjorken and E. A. Paschos, Phys. Rev. **185**, 1975 (1969).

are the diagrams which can be separated into two fast-moving parts joining together by vector mesons (here photons) only. Some typical diagrams of this category are shown in Fig. 1. Figure 1 describes the amplitude due to *pure* photon exchange without further interactions among the exchanged photons. The blobs appearing here are primitive pieces, i.e., they cannot be separated into two or more parts by cutting photon lines only, as demonstrated in Fig. 1. We now consider a subclass of diagrams in Fig. 1 in which we also ignore the EM interactions (radiative correction, etc.) within the hadronic blobs. As we shall see, summing over diagrams of this latter type leads to expressions identical to the operator droplet model conjectured by Chou and Yang.[1]

The purpose of introducing two types of interaction here is to provide a clear-cut separation between the mechanism for production of final particles and the interaction between the jets. As we shall see in more detail in Sec. IV, this kind of distinction is not possible for pure QED calculations.

In III, we showed that the amplitude for the diagram of Fig. 1 can be written, in the limit of large s, as

$$M=\tfrac{1}{2}s\int\left(\prod\frac{dq_-'}{4\pi}\right)A_{++\cdots+}(p_a',q')4\pi\delta(\sum q_-'-k_-')$$
$$\times\left(\prod\frac{dq_+''}{4\pi}\right)C_{--\cdots-}(p_c'',q'')4\pi\delta(\sum q_+''-k_+'')$$
$$\times\prod_i\left(\frac{d^2q_i}{(2\pi)^2}\frac{-ie^2}{\mathbf{q}_i^2+\mu^2}\right)(2\pi)^2\delta^2(\sum_i\mathbf{q}_i-\mathbf{k}),\quad(2.2)$$

where k is the momentum transfer. $A_{\mu\nu\cdots\sigma}(p',q')$ is the partial amplitude for the left-hand side of the graph of Fig. 1, evaluated in the standard frame (essentially the lab frame) of particle a, defined by

$$\begin{aligned}&p_{a+}'\equiv p_a'^0+p_a'^3=1\,,\\&p_{ai+}'\equiv p_{ai+}/p_{a+}\,,\quad 0<p_{ai+}'<1\\&\mathbf{p}_{ai}'\equiv\mathbf{p}_{ai}\,,\\&p_{ai-}'\equiv p_{ai}'^0-p_{ai}'^3\equiv p_{a+}p_{ai-}\,.\end{aligned}\quad(2.3)$$

The plus and minus appearing in (2.2) represent the four-vector indices 0+3 and 0−3. The variables p_+' and $\mathbf{p}'$, the fractional longitudinal momentum and the transverse momentum, form a very convenient parametrization for describing high-energy scattering. Readers are invited to consult II and III for more detailed kinematics of this infinite-momentum frame.

Similarly, $C_{\mu\nu\cdots\sigma}(p'',q'')$ is the partial amplitude of the right-hand side of the graph of Fig. 1, evaluated in the standard frame of particle c:

$$\begin{aligned}&p_{c-}''\equiv p_c''^0-p_c''^3=1\,,\\&p_{ci-}''\equiv p_{ci-}/p_{c-}\,,\quad 0<p_{ci-}''<1\\&\mathbf{p}_{ci}''\equiv\mathbf{p}_{ci}\,,\quad p_{ci+}''\equiv p_{c-}p_{ci+}\,.\end{aligned}\quad(2.4)$$

The momentum variables for the exchange photon can be chosen as q_+'', $\mathbf{q}'=\mathbf{q}''$, and q_-'. The other combinations, $q_+'=q_+''/s$ and $q_-''=q_-'/s$, vanish at $s=\infty$.

The amplitude $A_{\mu\nu\cdots\sigma}(p_a,q)$ is a generalized vertex function. First, we wish to point out that the above amplitude is related to the matrix element of the Heisenberg operators j_μ for the strong interaction alone through

$$\int(\prod_j d^4x_j)e^{-i\sum_i q_i\cdot x_i}\langle A|T(j_\mu(x_1)\cdots j_\lambda(x_N))|a\rangle$$
$$=(2\pi)^4\delta^4(p_a+q-\sum p_{ai})\times\sum_{\substack{\text{all possible}\\ N\text{-photon subgraphs}}}A_{\mu\nu\cdots\lambda}(p_a,q)\,,\quad(2.5)$$

where $q=\sum q_j$, and a and A are shorthand notations for initial particle a and its products A. We shall sometimes refer to A as jet A.[8] After including *all* N-photon exchange diagrams, we also find that Eq. (2.2) reduces to

$$M^{(N)}=\tfrac{1}{2}s\sum_{\substack{\text{all possible}\\ N\text{-photon diagrams}}}\int\left(\prod\frac{dq_-'}{4\pi}\right)A_{++\cdots+}(p_a',q')4\pi\delta(\sum q_-'-k_-')\left(\prod\frac{dq_+''}{4\pi}\right)C_{--\cdots-}(p_c'',q'')4\pi\delta(\sum q_+''-k_+'')$$
$$\times\prod_i\left(\frac{d^2q_i}{(2\pi)^2}\frac{-ie^2}{\mathbf{q}_i^2+\mu^2}\right)(2\pi)^2\delta^2(\sum\mathbf{q}_i-\mathbf{k})$$
$$=\tfrac{1}{2}s\frac{1}{N!}\int\left(\prod\frac{dq_-'}{4\pi}\right)\Big[\sum_{\substack{\text{all}\\ \text{subgraphs}}}A_{++\cdots+}(p_a',q')\Big]4\pi\delta(\sum q_-'-k_-')\left(\prod\frac{dq_+''}{4\pi}\right)\Big[\sum_{\substack{\text{all}\\ \text{subgraphs}}}C_{--\cdots-}(p_b'',q'')\Big]$$
$$\times4\pi\delta(\sum q_+''-k_+'')\prod_i\left(\frac{d^2q_i}{(2\pi)^2}\frac{-ie^2}{\mathbf{q}_i^2+\mu^2}\right)(2\pi)^2\delta^2(\sum\mathbf{q}_i-\mathbf{k})\,.\quad(2.6)$$

[8] The one-particle states are normalized covariantly. $\langle p'|p\rangle=(2\pi)^3 2E\delta^3(p'-p)$ for bosons and $(2\pi)^3(E/m)\delta^3(p'-p)$ for fermions.

By including all possible subgraphs in both A and C, we actually count diagrams with exchange photons labeled differently as different diagrams. The factor $1/N!$ is included to compensate for the overcounting.

Now, the contribution for the subgraph A can be reduced to

$$(2\pi)^4\delta^4(p_a'+k'-\sum p_{ai}')\int\left(\prod\frac{dq_-'}{4\pi}\right)\times\sum_{\substack{\text{all}\\ \text{subgraphs}}} A_{++\cdots+}(p_a',q')|_{q_+'=0}4\pi\delta(\sum q_-'-k_-')$$

$$=\int(\prod_j d^4x_j)\left(\prod_{\text{loops}}\frac{dq_-'}{4\pi}\right)e^{-i\Sigma_i q_i'x_i'}\times\langle A'|T(j_+(x_1')\cdots j_+(x_N'))|a'\rangle, \quad (2.7)$$

where A' and a' label jet A and particle a in the standard frame. By the use of

$$q'x'|_{q_+'=0}=\tfrac{1}{2}q_-'x_+'-\mathbf{q}'\cdot\mathbf{x}'$$

it is easy to carry out the q_-' (loop) integrals, giving

$$\prod_{\text{oops}}\int\frac{dq_-'}{4\pi}e^{-i\Sigma_i q_i'x_i'}\Big|_{q_+'=0}=\int dx_+'\,e^{i\mathbf{q}_i\cdot\mathbf{x}_i-ik_-'x_+'/2}\prod_i\delta(x_{i+}'-x_+'). \quad (2.8)$$

The δ functions in (2.8) ensure that the $j_+(x_i')$ appearing in (2.7) are at equal x_+. It is shown in the Appendix that the plus components of the EM current commute among themselves on the light cone $x_+=$ const. Hence the T product in (2.7) is the same as an ordinary product. This is important because we can now carry out the remaining integrations without worrying about the T ordering:

$$\text{left-hand side of (2.7)}=4\pi\delta(p_{a-}'+k_-'-\sum p_{ai-}')\times\langle A'|\sigma_+(\mathbf{q}_1)\cdots\sigma_+(\mathbf{q}_N)|a'\rangle, \quad (2.9)$$

where

$$\sigma_+(\mathbf{x})=\tfrac{1}{2}\int dx_-\,j_+(x_+=0,\mathbf{x},x_-), \quad (2.10)$$

$$\sigma_+(\mathbf{q})=\int d^2x\,e^{i\mathbf{q}\cdot\mathbf{x}}\sigma_+(\mathbf{x}). \quad (2.11)$$

The operator $\sigma_+(\mathbf{x})$ is essentially the $\sigma(\mathbf{x})$ introduced by Lee.[2] It obeys the simple relations

$$[\sigma_+(\mathbf{x}_1),\sigma_+(\mathbf{x}_2)]=0,$$

$$\int d^2x\,\sigma_+(\mathbf{x})=Q\ \text{(charge operator)},$$

and the TCP transformation properties as demonstrated by Lee.

An analogous result holds for the partial amplitude $C_{--\cdots-}(p_c'',q'')$:

$$(2\pi)^4\delta^4(p_c''-k''-\sum p_{ci}'')\times\int\left(\prod\frac{dq_+''}{4\pi}\right)C_{--\cdots-}(p_c'',q'')|_{q_-''=0}4\pi\delta(\sum q_+''-k_+)$$

$$=4\pi\delta(p_{c+}''-k_+''-\sum p_{ci}'')\times\langle C''|\sigma_-(-\mathbf{q}_1)\cdots\sigma_-(-\mathbf{q}_N)|c''\rangle, \quad (2.12)$$

with

$$\sigma_-(\mathbf{y})=\tfrac{1}{2}\int dy_+\,j_-(y_+,\mathbf{y},y_-=0), \quad (2.13)$$

$$\sigma_-(\mathbf{q})=\int d^2y\,e^{i\mathbf{q}\cdot\mathbf{y}}\sigma_-(\mathbf{y}). \quad (2.14)$$

c and C represent particle c and its products (jet C). The double prime on a symbol indicates that the quantity is measured in the standard frame of particle c. Putting Eqs. (2.9)–(2.14) together and performing k integrations, we find

$$M^{(N)}(2\pi)^4\delta(p_{a+}'-\sum p_{ai+}')\delta(p_{c-}''-\sum p_{ci-}'')\delta^2(\mathbf{p}_a+\mathbf{p}_c-\sum\mathbf{p}_{ai}-\sum\mathbf{p}_{ci})$$
$$=\tfrac{1}{2}s\frac{1}{N!}\int\prod_i\left(\frac{d^2q_i}{(2\pi)^2}\frac{-ie^2}{\mathbf{q}_i^2+\mu^2}\right)\langle A'|\sigma_+(\mathbf{q}_1)\cdots\sigma_+(\mathbf{q}_N)|a'\rangle\langle C''|\sigma_-(-\mathbf{q}_1)\cdots\sigma_-(-\mathbf{q}_N)|c''\rangle$$
$$=\tfrac{1}{2}s\frac{1}{N!}\langle A',C''|\left[\int\frac{d^2q}{(2\pi)^2}\sigma_+(\mathbf{q})\frac{-ie^2}{\mathbf{q}^2+\mu^2}\sigma_-(\mathbf{q})\right]^N|a',c''\rangle. \quad (2.15)$$

In the last expression, it is understood that the operator σ_+ (σ_-) has only matrix elements between the states associated with particle a (or particle c). The state $|a',c''\rangle=|a'\rangle\otimes|c''\rangle$ is a shorthand notation for a state with particles a and c in their respective standard frames.

The total amplitude of Fig. 1 can be obtained from $M^{(N)}$ by summing over all N, giving

$$M(2\pi)^4\delta(p_{a+}'-\sum p_{ai+}')\delta(p_{c-}''-\sum p_{ci-}'')\delta^2(\mathbf{p}_a+\mathbf{p}_c-\sum\mathbf{p}_{ai}-\sum\mathbf{p}_{ci})$$
$$=\tfrac{1}{2}s\langle A',C''|\exp\left[\int\frac{d^2q}{(2\pi)^2}\sigma_+(\mathbf{q})\frac{-ie^2}{\mathbf{q}^2+\mu^2}\sigma_-(-\mathbf{q})\right]-1|a',c''\rangle$$
$$=\tfrac{1}{2}s\langle A',C''|\exp\left[-ie^2\int d^2xd^2y\,\sigma_+(\mathbf{x})V(\mathbf{x}-\mathbf{y})\sigma_-(\mathbf{y})\right]-1|a',c''\rangle, \quad (2.16)$$

with

$$V(\mathbf{x})=\int\frac{d^2q}{(2\pi)^2}e^{i\mathbf{q}\cdot\mathbf{x}}\frac{1}{\mathbf{q}^2+\mu^2}. \tag{2.17}$$

The exponentiation of a convolution of two operator densities is precisely the structure of the operator droplet model.

To obtain the original form of the model,[1] we follow the procedure developed by Lee. Introducing

$$2\pi\delta(p_{f+}-p_{i+})\langle\sigma_+(\mathbf{x}_1+\mathbf{z})\cdots\sigma_+(\mathbf{x}_N+\mathbf{z})\rangle_{fi}\equiv\int\frac{d^2k}{(2\pi)^2}e^{-i\mathbf{k}\cdot\mathbf{z}}\langle p_f,\tfrac{1}{2}\mathbf{k}|\sigma_+(\mathbf{x}_1)\cdots\sigma_+(\mathbf{x}_N)|p_i,-\tfrac{1}{2}\mathbf{k}\rangle,$$

$$\langle p_f,\tfrac{1}{2}\mathbf{k}|\sigma_+(\mathbf{x}_1)\cdots\sigma_+(\mathbf{x}_N)|p_i,-\tfrac{1}{2}\mathbf{k}\rangle=2\pi\delta(p_{f+}-p_{i+})\int d^2z\, e^{i\mathbf{k}\cdot\mathbf{z}}\langle\sigma_+(\mathbf{x}_1+\mathbf{z})\cdots\sigma_+(\mathbf{x}_N+\mathbf{z})\rangle_{fi} \tag{2.18}$$

and analogous equations for the σ_-'s, we have

$$M(2\pi)^4\delta(p_{a+}'-\textstyle\sum p_{ai+}')\delta(p_{c-}''-\sum p_{ci-}'')\delta^2(\mathbf{p}_a+\mathbf{p}_c-\sum\mathbf{p}_{ai}-\sum\mathbf{p}_{ci})=\tfrac{1}{2}s(2\pi)^2\delta(p_{a+}'-\sum p_{ai+}')\delta(p_{c-}''-\sum p_{ci-}'')$$
$$\times\int dzdz'\,e^{i\mathbf{k}\cdot\mathbf{z}-i\mathbf{k}'\mathbf{z}'}\left\langle\exp\left[-ie^2\int d^2xd^2y\,\sigma_+(\mathbf{x}+\mathbf{z})V(\mathbf{x}-\mathbf{y})\sigma_-(\mathbf{y}+\mathbf{z}')\right]-1\right\rangle_{A',C'';a',c''}. \tag{2.19}$$

After making the translations $\mathbf{x}+\mathbf{z}\rightarrow\mathbf{x}$ and $\mathbf{y}+\mathbf{z}'\rightarrow\mathbf{y}$, and carrying out one z integration for fixed $\mathbf{b}=\mathbf{z}'-\mathbf{z}$, we have

$$M_{A',C'';a',c''}(k)=\tfrac{1}{2}s\int d^2b\,e^{-i\mathbf{k}\cdot\mathbf{b}}\times\langle S(\mathbf{b})-1\rangle_{A',C'';a',c''}, \tag{2.20}$$

with

$$S(\mathbf{b})=\exp\left[-ie^2\int\sigma_+(\mathbf{x})V(\mathbf{x}-\mathbf{y}+\mathbf{b})\times\sigma_-(\mathbf{y})d^2xd^2y\right]. \tag{2.21}$$

Equation (2.20) is exactly the operator droplet model as conjectured by Chou and Yang.

III. ALTERNATIVE DERIVATION

We have found that the asymptotic amplitude due to the set of diagrams of Fig. 1 can be cast into a form suggested by the operator droplet model. Since the final answer is very simple, one expects that this result might be obtained more directly. Let us summarize the ingredients which enter into the derivation.

(1) The scattering amplitude factors into two parts, one associated with the target and one associated with the projectile. The large component of the momentum in each part (p_+ for particle a and its products and p_- for particle c and its products) is preserved during the scattering. These two parts are joined together by vector mesons only.

(2) The leading contribution of these diagrams comes from the plus components of the left-hand graph coupled with the minus components of the right-hand graph.

(3) The proper variables to use in describing the amplitudes are those measured in the frames moving with the particles. These are standard-frame variables for particle a and for particle c.

To give a simple derivation, we decompose the Hamiltonian into $H_0'+H_1'$, where H_0' consists of all kinematical terms as well as the strong interactions, and $H_1'=-\mathcal{L}_2'=ej^\mu A_\mu$ contains only the EM interaction. The S matrix, in an interaction representation, is given by Dyson's equation

$$S=T\exp\left(-ie\int d^4x\,j^\mu A_\mu\right). \tag{3.1}$$

The effective S matrix corresponding to Fig. 1 can be obtained from Eq. (3.1) by contracting out the Maxwell fields in the exponent, giving

$$S^{(\text{Fig. 1})}=T\exp\left[ie^2\int dxdy\,j_\mu^{(a)}(x)\times D_F(x-y)j_\mu^{(c)}(y)\right]. \tag{3.2}$$

Here $j_\mu^{(a)}$ represents the EM current interacting with particle a and jet A, and $j_\mu^{(c)}$ represents the EM current interacting with particle c and jet C. Remember that we have included strong interactions exactly within the hadronic blobs for jet A and jet C. For the particular set of diagrams studied here, the strong interactions among jet A and jet C do not mix. Hence, we can treat them separately.

In the Heisenberg representation for the strong interaction alone, the matrix element for the diagrams of Fig. 1 is

$$\langle A,C|T\exp\left[-ie^2\int d^4xd^4y\ j_\mu{}^{(a)}(x)\times D_F(x-y)j_\mu{}^{(c)}(y)\right]|a,c\rangle. \quad (3.3)$$

The final states A and C describe the jets produced from the incident particles a and c, respectively. Even though Eq. (3.3) is very similar in appearance to (2.16), these equations are in fact quite different. First, Eq. (3.3) contains a T product. Second, the s dependence of the amplitude is still implicit in (3.3).

To manifest the explicit behavior of the amplitude at $s\to\infty$, we make a Lorentz transformation for particle a and jet A from the c.m. frame to the standard frame of particle a:

$$|a\rangle=U_a{}^{-1}|a'\rangle,\quad \langle A|=\langle A'|U_a, \quad (3.4)$$

$$\begin{aligned} U_aj^{(a)\mu}(x)U_a{}^{-1}&=(\sqrt{s})j_+{}^{(a)}(x'), & \mu&=+\\ &=\mathbf{j}^{(a)}(x'), & \mu&=\perp\\ &=(1/\sqrt{s})j_-{}^{(a)}(x'), & \mu&=-, \end{aligned} \quad (3.5)$$

with

$$\begin{aligned} p_{a+}'&=(1/\sqrt{s})p_{a+}=1, & \mathbf{p}_a'&=\mathbf{p}_a, & p_{a-}'&=(\sqrt{s})p_{a-},\\ x_+'&=(1/\sqrt{s})x_+, & \mathbf{x}'&=\mathbf{x}, & x_-'&=(\sqrt{s})x_-. \end{aligned} \quad (3.6)$$

The momentum p and coordinate x are c.m. variables, as before. For simplicity, we assume that the states are normalized covariantly so that no additional kinematical terms arise during the Lorentz transformation. Similarly, we make a Lorentz transformation on particle c and jet C from the c.m. frame to standard frame c:

$$|c\rangle=U_c{}^{-1}|c''\rangle,\quad \langle C|=\langle C''|U_c,$$

$$\begin{aligned} U_cj^{(c)\mu}U_c{}^{-1}&=(1/\sqrt{s})j_+{}^{(c)}(y''), & \mu&=+\\ &=\mathbf{j}^{(c)}(y''), & \mu&=\perp\\ &=(\sqrt{s})j_-{}^{(c)}(y''), & \mu&=-, \end{aligned} \quad (3.7)$$

with

$$\begin{aligned} p_{c+}''&=(\sqrt{s})p_{c+}, & \mathbf{p}_c''&=\mathbf{p}_c, & p_{c-}''&=(1/\sqrt{s})p_{c-}=1,\\ y_+''&=(\sqrt{s})y_+, & \mathbf{y}''&=\mathbf{y}, & y_-''&=(1/\sqrt{s})y_-. \end{aligned} \quad (3.8)$$

After these transformations, the exponent appearing in Eq. (3.3) reduces asymptotically to

$$E=-\tfrac{1}{2}ie^2s\int d^4xd^4y\ j_+{}^{(a)}(x')D_F(x-y)j_-{}^{(c)}(y''). \quad (3.9)$$

The quantities x_+' and y_-'', which are of order $O(1/\sqrt{s})$, are Lorentz contracted. So are the quantities x_- and y_+ in the c.m. frame.[9] At the infinite-s limit, these quantities are contracted to zero, and may be ignored. Hence

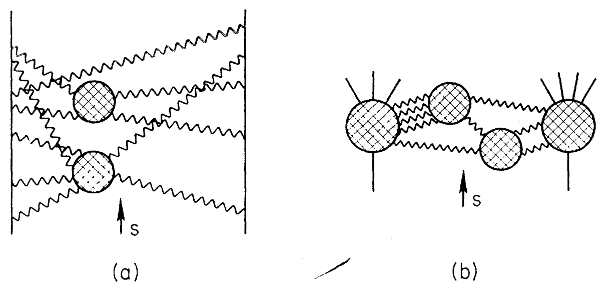

FIG. 2. Multiphoton-exchange diagrams with further photon-photon interactions. (a) Typical diagram without any vertex corrections on the incident fermion lines. (b) General diagram with two bubbles.

$$E=-\tfrac{1}{2}ie^2s\int\frac{1}{2\sqrt{s}}dx_+dx_-'d^2x\ j_\mu{}^{(a)}(x_+'=0,\mathbf{x},x_-')\times\frac{1}{2\sqrt{s}}dy_+''dy_-d^2y\ j_-{}^{(c)}(y_+'',\mathbf{y},y_-''=0)\times D_F(x_+,\mathbf{x}-\mathbf{y},-y_-). \quad (3.10)$$

Carrying out the x_+ and y_- integrations, we have

$$E=-ie^2\int\tfrac{1}{2}d^2xdx_-'\ j_+{}^{(a)}(x_+'=0,\mathbf{x},x_-')\times\tfrac{1}{2}dy_+''d^2y\ j_-{}^{(c)}(y_+'',\mathbf{y},y_-''=0)V(\mathbf{x}-\mathbf{y}). \quad (3.11)$$

Since the $j_+{}^{(a)}(x_+'=0,\mathbf{x},x_-')$'s [and $j_-{}^{(c)}(y_+'',\mathbf{y},y_-''=0)$] commute among themselves, the T product is the same as an ordinary product. Therefore, we can do the dx_-' and dy_+'' integrations without worrying about the T product, leading to

$$E=-ie^2\int d^2xd^2y\ \sigma_+(\mathbf{x})V(\mathbf{x}-\mathbf{y})\sigma_-(\mathbf{y}), \quad (3.12)$$

with σ_+ and σ_- defined in (2.10) and (2.13). Hence, the matrix element (3.3) reduces to

$$\langle A',C''|\exp\left[-ie^2\int d^2xd^2y\ \sigma_+(\mathbf{x})V(\mathbf{x}-\mathbf{y})\sigma_-(\mathbf{y})\right]\times|a',c''\rangle. \quad (3.13)$$

In terms of the invariant matrix, this is precisely Eq. (2.16).

IV. POSSIBLE GENERALIZATION OF MODEL

We have shown in previous sections that the operator droplet model may be viewed as the contribution due to a set of Feynman diagrams in Fig. 1. It is natural to ask about possible generalizations of the model if additional sets of diagrams are included.

[9] What is important here is that we can always ignore x_- in comparison with y_-, and y_+ in comparison with x_+. The relative magnitude of x_-, y_+ versus y_-, x_+ is independent of the particular reference frame (here the c.m. frame) that we are using.

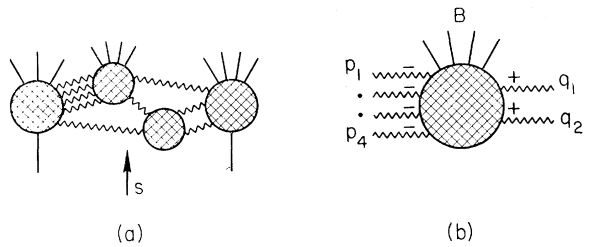

FIG. 3. (a) Diagram analogous to 2(a) but with evaporation particles from one bubble. (b) Evaporation bubble in more detail.

It is known that the diagrams of Fig. 1 are not the only set of leading diagrams at $s=\infty$. Diagrams with exchange photons interacting among themselves lead to a larger set of diagrams which are also large at $s=\infty$. Some typical diagrams of this larger category are shown in Fig. 2. These diagrams together with possible evaporation diagrams (Fig. 3) are, we believe, the only diagrams which are large at $s=\infty$.[10] They behave like $s(\ln s)^N$ at large s, where N is the number of primitive bubbles introduced in III. Readers are referred to this reference for details.

Diagrams in Figs. 2 and 3 will no longer give the simple fixed-s^1 behavior. Actually, this is important, since the fixed-s^1 behavior violates unitarity.[11] If we take this larger set of diagrams seriously, we find that the droplet model must be modified. Among other possible modifications (see Sec. V), the s-independent potential appearing in the original operator droplet model might be replaced by an s-dependent potential $V(s,\mathbf{x})$. To see how this fits in naturally, we consider the diagram of Fig. 2(a). It is shown in III that the over-all amplitude for this type of diagram is

$$\tfrac{1}{2}s\frac{\delta_{a'a}}{m}\frac{\delta_{c'c}}{m}\int d^2b\, e^{-i\mathbf{k}\cdot\mathbf{b}}[e^{i\chi(s,\mathbf{b})}-1], \qquad (4.1)$$

with

$$i\chi(s,\mathbf{b})=\int\frac{d^2k}{(2\pi)^2}e^{i\mathbf{k}\cdot\mathbf{b}}F(s,\mathbf{k}), \qquad (4.2)$$

$$F(s,\mathbf{k})=\sum(\text{all connected diagrams with momentum transfer } k). \qquad (4.3)$$

A direct calculation from the operator droplet model, in analogy with Lee, gives

$$V(s,\mathbf{x})=-\chi(s,\mathbf{x}) = \text{Fourier transform of } iF(s,\mathbf{k}). \qquad (4.4)$$

An s-dependent potential obtained by including all connected diagrams should be an important generalization of the original droplet model.

The geometrical meaning of this modification is that the "opaqueness" of the droplet is energy dependent. Hence, it leads to a slow s dependence in the forward differential cross section.[12] This is also the physical picture suggested by the Regge model.

Another important class of diagrams that we would like to discuss is that associated with the evaporation of particles from the bubbles. These evaporation particles have a dp_+/p_+ distribution in momentum space, and are qualitatively different from the particles emitted from blobs A and C. It is physically sound to identify jet A and jet C emitted from blobs A and C as fragments of the target and the projectile. For evaporation particles, however, there is a *uniform* distribution in $\ln p_+$ space. The momentum spectrum of these particles spans the entire available range, starting all the way from p_a to p_c. As s increases, the available range of the momentum spectrum increases. Nevertheless, its distribution remains the same (uniform distribution) in $\ln p_+$ space. For this reason, they should not be classified as fragments.[13] The partial amplitude for the evaporation of particles B in Fig. 3(b) can be computed in an analogous way as

$$(4\pi)^2\delta(\textstyle\sum p_+)\delta(\sum q_-)\times\displaystyle\int\prod(\tfrac{1}{2}d^2x dx_-)\prod(\tfrac{1}{2}dy_+d^2y)e^{\Sigma i\mathbf{q}\cdot\mathbf{x}-\Sigma i\mathbf{p}\cdot\mathbf{y}} \times\langle B|T[j_+(x_{1+}=0,\mathbf{x}_1,x_{1-})\cdots j_-(y_{1+},\mathbf{y}_1,y_{1-}=0)\cdots]|0\rangle. \qquad (4.5)$$

This result does not reduce simply to products of σ_+ and σ_- because $j_+(x_+=0,\mathbf{x},x_-)$ and $j_-(y_+,\mathbf{y},y_-=0)$ do not commute.[14]

V. QUANTUM ELECTRODYNAMICS

The separation of interactions into an interaction without fundamental vector particles and an EM interaction mediated by photon (a vector particle) exchange no longer makes sense in pure QED. Even though it is still possible to classify a diagram according to its primitive components, as we did in III, summation over diagrams analogous to Fig. 1 does not lead to an expression suggested by the original operator droplet model. This can be understood from the observation

[10] These are the diagrams which have the following nice properties: (1) The infinite momenta p_{a+} and p_{c-} have separate pathways, and (2) the two infinite parts are linked by photons only. See II for detailed discussion. Note that even though these diagrams give rise to leading contribution to each order of perturbatheory, it is not clear that the sum of all these diagrams is still leading. A recent calculation [S. J. Chang and T. M. Yan (unpublished)] indicates that diagrams with scalar-meson (or Dirac particle) exchange can give rise to an amplitude comparable in magnitude to those obtained from pure vector exchange.

[11] V. N. Gribov and I. Ya Pomeranchuk, Phys. Letters **2**, 239 (1962).

[12] Recent experiments on p-p scattering seem to support such a slow s dependence. See G. G. Beznogikh *et al.*, Phys. Rev. Letters **30B**, 274 (1969).

[13] The particles emitted from a single bubble are kinematically related. Whether these particles are responsible for a "pionization" effect will certainly depend on how one interprets the data.

[14] By identifying T as x_+ (or x_-) ordering, we can move all j_+ (or j_-) together and reduce them to σ_+ (or σ_-). However, one cannot do this simultaneously for both j_+ and j_-.

that the generalized vertex function

$$\int \left(\prod dx\right) e^{-i\sum q_i\cdot x_i}\langle A\,|\,T(j_\mu(x_1)\cdots j_\lambda(x_N))\,|\,a\rangle$$

$$\equiv(2\pi)^4\delta^4(p_a+q-\sum p_{ai})A_{\mu\nu\cdots\lambda}{}^{(\mathrm{B.B.})}(p_a,q) \quad (5.1)$$

will give rise to an amplitude which contains all possible N-photon diagrams, including both the primitive and the nonprimitive graphs. This amplitude is denoted by a black box (B.B.) in Fig. 4. Therefore, a partial sum of the graphs, such as Fig. 1, is not sufficient in the present case to generate an expression consistent with an operator droplet model.

The above considerations indicate that a sum over all possible photon-exchange diagrams between two black boxes in Fig. 5 should lead to an operator droplet model analogous to the result developed in Secs. II and III. Since the black box contains all kinds of nonprimitive graphs, the union of two such black boxes should generate all possible leading graphs, and hence the leading amplitude at $s=\infty$. The amplitude for process $a+c\to A+C$ (i.e., jet A and jet C) obeys relations (2.6) and (2.16) provided that we replace the expressions $\sum A_{++\ldots+}$ and $\sum C_{--\ldots-}$ in (2.6) by the corresponding expressions $A_{++\ldots+}{}^{(\mathrm{B.B.})}$ and $C_{--\ldots-}{}^{(\mathrm{B.B.})}$ for the black boxes. Hence, for N-photon exchange, we have

$$M^{(N)}=\tfrac{1}{2}s\frac{1}{N!}\int\left(\prod\frac{dq_-{}'}{4\pi}\right)$$
$$\times A_{++\ldots+}{}^{(\mathrm{B.B.})}(p_a{}',q')4\pi\delta(\sum q_-{}'-k_-{}')$$
$$\times\left(\prod\frac{dq_+{}''}{4\pi}\right)C_{--\ldots-}{}^{(\mathrm{B.B.})}(p_c{}'',q'')4\pi\delta(\sum q_+{}''-k_+{}'')$$
$$\times\prod_i\left(\frac{d^2q_i}{(2\pi)^2}\frac{-ie^2}{\mathbf{q}_i{}^2+\mu^2}\right)(2\pi)^2\delta^2(\sum\mathbf{q}_i-\mathbf{k}). \quad (5.2)$$

For the over-all amplitude, we have

$$M(2\pi)^4\delta(p_{a+}{}'-\sum p_{ai+}{}')\delta(p_{c-}{}''-\sum p_{ci-}{}'')$$
$$\times\delta^2(\mathbf{p}_a+\mathbf{p}_c-\sum\mathbf{p}_{ai}-\sum\mathbf{p}_{ci})=\tfrac{1}{2}s\langle A',C''|$$
$$\times\exp\left[-ie^2\int d^2xd^2y\,\sigma_+(\mathbf{x})V(\mathbf{x}-\mathbf{y})\sigma_-(\mathbf{y})\right]-1\,|\,a',c''\rangle. \quad (5.3)$$

To make these expressions more precise and hence more useful, we would like to study the black-box contribution carefully. Strictly speaking, the perturbation expansion of (5.1), or equivalently the black-box expression $A^{(\mathrm{B.B.})}$, does *not* approach a finite limit at $s=\infty$. (Of course, this does not exclude the possibility that the over-all sum of the perturbation series may converge to a finite limit. However, we shall not investigate this possibility here.) The lowest-order (e^6) diagrams which lead to this divergence difficulty are

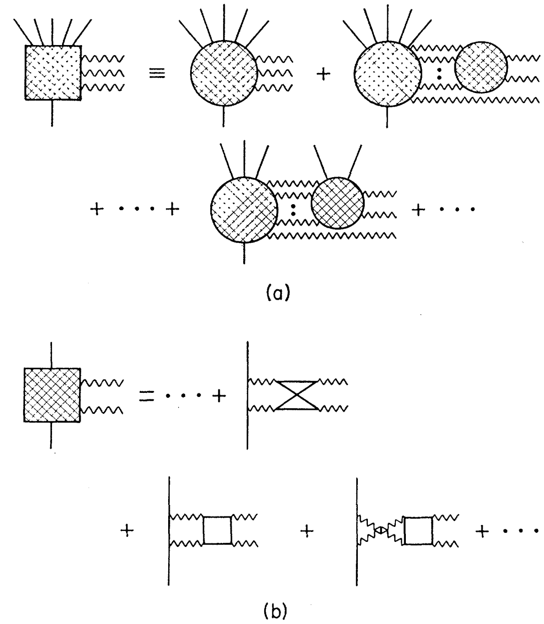

FIG. 4. (a) Diagrammatic expansion of a typical black box. (b) Lowest-order processes which contribute to the logarithmic divergence of the black box.

due to the photon-photon interaction, as shown in Fig. 4(b). These diagrams are, in fact, the lowest-order nonprimitive diagrams. Following the argument given in III, it can be shown that the contribution to Fig. 4(b) goes like $\ln s_1$ at large s_1, where s_1 is the energy squared for the incident electron (of momentum p_a) measured in the reference frame. In our language (see Sec. II of Paper III), $\ln s_1$ is a measure of the available $\ln p_+$ phase space in which the electron loop can slide freely. If we cut the diagram of Fig. 4(b) horizontally, we find that the intermediate state consists of an e^+e^- pair. This e^+e^- pair is the simplest evaporation process which we discussed in Sec. III. The divergence in (5.1) may be viewed as due to the presence of these virtual evaporation particles in the intermediate state, and reflects the increase of the available phase space as s_1 increases.

Since the subenergy s_1 depends on the particular reference frame, the same arbitrariness will appear in the evaluation of the black box in the graph of Fig. 4. This sounds unpleasant because the physical amplitude should not depend on the particular reference frame being used. However, as we shall see, the dependence on the reference frame is only superficial. This dependence will disappear if graphs related to one another by

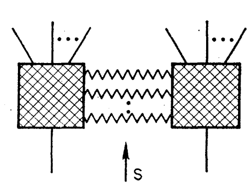

FIG. 5. Union of two black-box diagrams. This symbolic diagram contains all leading Feynman diagrams in QED.

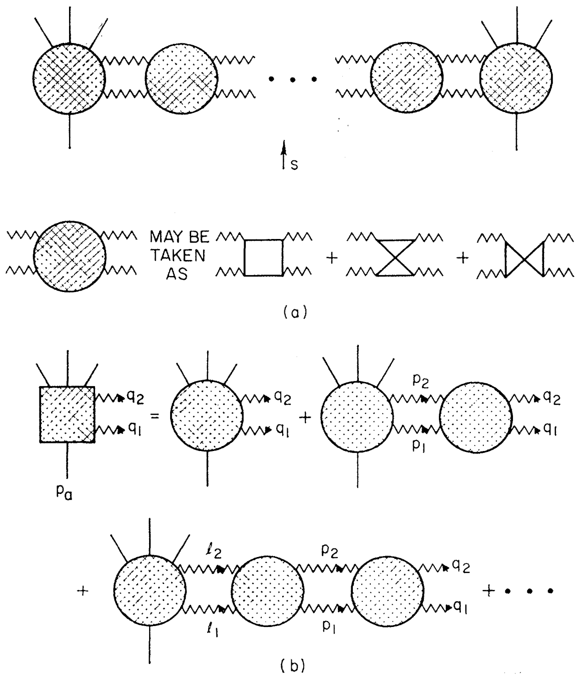

FIG. 6. (a) Diagram with repetition of bubbles in the t channel. (b) Relevant partial amplitudes in a black-box expansion.

different partitions are all added together. This is very similar in spirit to the verification of gauge invariance in the usual QED calculations. In general, individual diagrams are not gauge invariant. However, when diagrams with photon vertices permuted in all possible ways on a charged line are included, a gauge-invariant result is always obtained.

In the following, we wish to work out a few examples by means of expression (5.2) [or, equivalently, (5.3)] to reproduce QED perturbation results obtained so far.

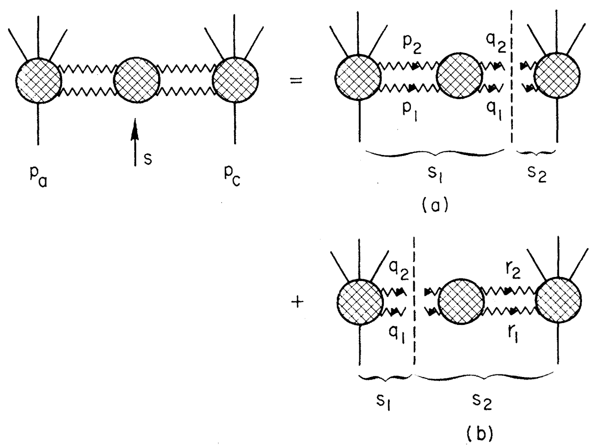

FIG. 7. Diagrams (a) and (b) are special cases of Fig. 5. The subgraphs on one side of the dashed line belong to a black box. Similarly, the subgraphs on the other side of the line belong to a different black box. The sum of (a) and (b) gives rise to a reference-frame-independent result.

In particular, we would like to demonstrate how a reference-frame-independent result emerges and how the correct $(\ln s)^N$ behavior is recovered.

A. Repetition of Bubbles in t Channel

The first example that we wish to work out is the repetition of bubbles in the t channel, shown in Fig. 6(a). The relevant parts of the left-hand black box with two external photons are given in Fig. 6(b). The partial amplitudes for these processes in the black box can be computed by means of the method developed in III, giving

$$\begin{aligned}\int \frac{dq_-'}{4\pi} A_{++}^{(\mathrm{B.B.})}(p_a',q') &= I_a(\mathbf{q}) + \frac{\ln s_1}{4\pi}\int \frac{d^2p}{(2\pi)^2} I_a(\mathbf{p}) J(\mathbf{p},\mathbf{q}) \frac{-ie^2}{\mathbf{p}_1^2+\mu^2}\,\frac{-ie^2}{\mathbf{p}_2^2+\mu^2} \\ &\quad + \frac{1}{2!}\left(\frac{\ln s_1}{4\pi}\right)^2 \int \frac{d^2l}{(2\pi)^2}\,\frac{d^2p}{(2\pi)^2} I_a(\mathbf{l}) J(\mathbf{l},\mathbf{p}) J(\mathbf{p},\mathbf{q}) \\ &\quad \times \frac{-ie^2}{\mathbf{l}_1^2+\mu^2}\,\frac{-ie^2}{\mathbf{l}_2^2+\mu^2}\,\frac{-ie^2}{\mathbf{p}_1^2+\mu^2}\,\frac{-ie^2}{\mathbf{p}_2^2+\mu^2} + \cdots, \end{aligned} \quad (5.4)$$

where I_a and I_c are impact factors for $a \to A$ and $c \to C$, and $J(\mathbf{p},\mathbf{q})$ is the loop contribution introduced in III. Similarly, we can compute the right-hand black box:

$$\begin{aligned}\int \frac{dq_+''}{4\pi} C_{-,-}^{(\mathrm{B.B.})}(p_c'',q'') &= I_c(\mathbf{q}) + \frac{\ln s_2}{4\pi}\int \frac{d^2r}{(2\pi)^2} J(\mathbf{q},\mathbf{r}) I_c(\mathbf{r}) \frac{-ie^2}{\mathbf{r}_1^2+\mu^2}\,\frac{-ie^2}{\mathbf{r}_2^2+\mu^2} \\ &\quad + \frac{1}{2!}\left(\frac{\ln s_2}{4\pi}\right)^2 \int \frac{d^2r}{(2\pi)^2}\,\frac{d^2t}{(2\pi)^2} J(\mathbf{q},\mathbf{r}) J(\mathbf{r},\mathbf{t}) I_c(\mathbf{t}) \\ &\quad \times \frac{-ie^2}{\mathbf{r}_1^2+\mu^2}\,\frac{-ie^2}{\mathbf{r}_2^2+\mu^2}\,\frac{-ie^2}{\mathbf{t}_1^2+\mu^2}\,\frac{-ie^2}{\mathbf{t}_2^2+\mu^2} + \cdots, \end{aligned} \quad (5.5)$$

where s_2 is the subenergy for particle c in the same reference frame. Simple kinematics tells us that, as $s_{1,2} \to \infty$,[15]

$$\ln s_1 + \ln s_2 \approx \ln s. \quad (5.6)$$

In our language, this is simply the additivity of the $\ln p_+$ phase space introduced in III.

The full amplitude is obtained by gluing together the right- and left-hand black boxes through (5.2). The simplest two-photon exchange part without any bubbles

[15] This relation can be obtained as follows: Let p_a', p_a, and p_a'' be the momenta of particle a in the target, the reference, and the projectile frame; then $\ln s_1 \approx \ln p_{a+}' - \ln p_{a+}$, $\ln s_2 \approx \ln p_{a+} - \ln p_{a+}''$, and $\ln s \approx \ln p_{a+}' - \ln p_{a+}''$. The relation $\ln s_1 + \ln s_2 = \ln s$ then follows. This type of relation is well known in multiperipheral processes.

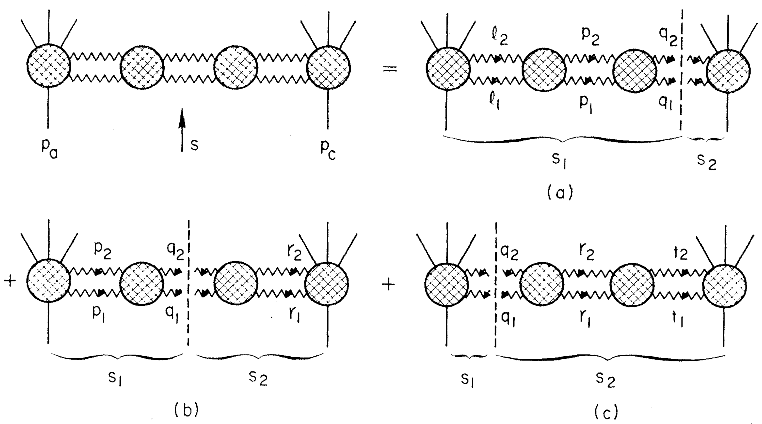

FIG. 8. Same as Fig. 7 with two linked bubbles.

gives

$$\tfrac{1}{2}s\frac{1}{2!}\int\frac{d^2q}{(2\pi)^2}I_a(\mathbf{q})I_c(\mathbf{q})\frac{-ie^2}{\mathbf{q}_1^2+\mu^2}\frac{-ie^2}{\mathbf{q}_2^2+\mu^2},\qquad(5.7)$$

which is trivially correct. Each of the factors in (5.7) is reference-frame independent, as is their product.

The first interesting case comes from the single-bubble amplitude. It corresponds to the coupling of a one-bubble contribution from one black box to the no-bubble contribution of the other. Diagrammatically, it is shown in Fig. 7. The contributions from Figs. 7(a) and 7(b) can be obtained by multiplying the corresponding terms in (5.4) and (5.5), giving

$$\tfrac{1}{2}s\frac{1}{2!}\frac{\ln s_1}{4\pi}\int\frac{d^2p}{(2\pi)^2}\frac{d^2q}{(2\pi)^2}I_a(\mathbf{p})J(\mathbf{p},\mathbf{q})I_c(\mathbf{q})\times\frac{-ie^2}{\mathbf{p}_1^2+\mu^2}\frac{-ie^2}{\mathbf{p}_2^2+\mu^2}\frac{-ie^2}{\mathbf{q}_1^2+\mu^2}\frac{-ie^2}{\mathbf{q}_2^2+\mu^2}\qquad(5.8\text{a})$$

and

$$\tfrac{1}{2}s\frac{1}{2!}\frac{\ln s_2}{4\pi}\int\frac{d^2q}{(2\pi)^2}\frac{d^2r}{(2\pi)^2}I_a(\mathbf{q})J(\mathbf{q},\mathbf{r})I_c(\mathbf{r})\times\frac{-ie^2}{\mathbf{q}_1^2+\mu^2}\frac{-ie^2}{\mathbf{q}_2^2+\mu^2}\frac{-ie^2}{\mathbf{r}_1^2+\mu^2}\frac{-ie^2}{\mathbf{r}_2^2+\mu^2},\qquad(5.8\text{b})$$

respectively. By adding together these two pieces and making use of (5.6), we obtain

$$\tfrac{1}{4}s\frac{\ln s}{4\pi}\int\frac{d^2p}{(2\pi)^2}\frac{d^2q}{(2\pi)^2}I_a(\mathbf{p})J(\mathbf{p},\mathbf{q})I_c(\mathbf{q})\times\frac{-ie^2}{\mathbf{p}_1^2+\mu^2}\frac{-ie^2}{\mathbf{p}_2^2+\mu^2}\frac{-ie^2}{\mathbf{q}_1^2+\mu^2}\frac{-ie^2}{\mathbf{q}_2^2+\mu^2}.\qquad(5.9)$$

Even though each of the individual terms is frame dependent, their sum is not. The final result agrees also with earlier calculations.

To demonstrate that the result holds for multibubble amplitudes, let us work out the diagrams of Fig. 8, which involve the repetition of two bubbles. The contributions due to diagrams 8(a), 8(b), and 8(c) are

$$\left(\frac{s}{2\cdot 2!}\right)\frac{1}{2!}\left(\frac{\ln s_1}{4\pi}\right)^2\int\frac{d^2l}{(2\pi)^2}\frac{d^2p}{(2\pi)^2}\frac{d^2q}{(2\pi)^2}\times I_a(\mathbf{l})J(\mathbf{l},\mathbf{p})J(\mathbf{p},\mathbf{q})I_c(\mathbf{q})\times\frac{-ie^2}{\mathbf{l}_1^2+\mu^2}\frac{-ie^2}{\mathbf{l}_2^2+\mu^2}\frac{-ie^2}{\mathbf{p}_1^2+\mu^2}\frac{-ie^2}{\mathbf{p}_2^2+\mu^2}\times\frac{-ie^2}{\mathbf{q}_1^2+\mu^2}\frac{-ie^2}{\mathbf{q}_2^2+\mu^2},\qquad(5.10\text{a})$$

$$\left(\frac{s}{2\cdot 2!}\right)\frac{\ln s_1}{4\pi}\frac{\ln s_2}{4\pi}\int\frac{d^2p}{(2\pi)^2}\frac{d^2q}{(2\pi)^2}\frac{d^2r}{(2\pi)^2}\times I_a(\mathbf{p})J(\mathbf{p},\mathbf{q})J(\mathbf{q},\mathbf{r})I_c(\mathbf{r})\times\frac{-ie^2}{\mathbf{p}_1^2+\mu^2}\frac{-ie^2}{\mathbf{p}_2^2+\mu^2}\frac{-ie^2}{\mathbf{q}_1^2+\mu^2}\frac{-ie^2}{\mathbf{q}_2^2+\mu^2}\times\frac{-ie^2}{\mathbf{r}_1^2+\mu^2}\frac{-ie^2}{\mathbf{r}_2^2+\mu^2},\qquad(5.10\text{b})$$

and

$$\left(\frac{s}{2\cdot 2!}\right)\frac{1}{2!}\left(\frac{\ln s_2}{4\pi}\right)^2\int\frac{d^2q}{(2\pi)^2}\frac{d^2l}{(2\pi)^2}\frac{d^2t}{(2\pi)^2}\times I_a(\mathbf{q})J(\mathbf{q},\mathbf{l})J(\mathbf{l},\mathbf{t})I_c(\mathbf{t})\times\frac{-ie^2}{\mathbf{q}_1^2+\mu^2}\frac{-ie^2}{\mathbf{q}_2^2+\mu^2}\frac{-ie^2}{\mathbf{l}_1^2+\mu^2}\frac{-ie^2}{\mathbf{l}_2^2+\mu^2}\times\frac{-ie_2}{\mathbf{t}_1^2+\mu^2}\frac{-ie^2}{\mathbf{t}_2^2+\mu^2},\qquad(5.10\text{c})$$

respectively. Each of the above expressions contains a frame-dependent factor multiplied by a common frame-independent basic term. Adding all three expressions together, we are led to a frame-independent factor,

$$\frac{1}{2!}\left(\frac{\ln s_1}{4\pi}\right)^2+\left(\frac{\ln s_1}{4\pi}\right)\left(\frac{\ln s_2}{4\pi}\right)+\frac{1}{2!}\left(\frac{\ln s_2}{4\pi}\right)^2=\frac{1}{2!}\left(\frac{\ln s_1+\ln s_2}{4\pi}\right)^2=\frac{1}{2!}\left(\frac{\ln s}{4\pi}\right)^2, \tag{5.11}$$

and hence to a final expression,

$$\tfrac{1}{4}s\frac{1}{2!}\left(\frac{\ln s}{4\pi}\right)^2\int\frac{d^2l}{(2\pi)^2}\frac{d^2p}{(2\pi)^2}\frac{d^2q}{(2\pi)^2}I_a(\mathbf{l})J(\mathbf{l},\mathbf{p})J(\mathbf{p},\mathbf{q})I_c(\mathbf{q})\frac{-ie^2}{\mathbf{l}_1^2+\mu^2}\frac{-ie^2}{\mathbf{l}_2^2+\mu^2}\frac{-ie^2}{\mathbf{p}_1^2+\mu^2}\frac{-ie^2}{\mathbf{p}_2^2+\mu^2}\frac{-ie^2}{\mathbf{q}_1^2+\mu^2}\frac{-ie^2}{\mathbf{q}_2^2+\mu^2}. \tag{5.12}$$

Equation (5.12) coincides with our previous calculation. The generalization of the present result to iteration of N bubbles is straightforward.

B. Iteration of Bubbles in s Channel

As a final example, we work out the iteration of two bubbles in the s channel. We shall omit most of the algebra because it is similar to what was used in example A. The diagram that we are dealing with is the e^-e^- scattering amplitude in Fig. 9. The relevant parts in the black box are shown in Fig. 10. This contribution can be worked out as

$$\int\prod\frac{dq_-'}{4\pi}A^{(\text{B.B.})}(p_a',q')=\frac{\delta_{a'a}}{m}+\frac{\delta_{a'a}}{m}\left(\frac{\ln s_1}{4\pi}\right)$$
$$\times\left[\int\frac{d^2p_1d^2p_2}{(2\pi)^4}J(\mathbf{p}_1,\mathbf{p}_2;\mathbf{q}_1\mathbf{q}_2)(2\pi)^2\delta^2(\mathbf{p}_1+\mathbf{p}_2-\mathbf{q}_{12})\frac{-ie^2}{\mathbf{p}_1^2+\mu^2}\frac{-ie^2}{\mathbf{p}_2^2+\mu^2}+[\text{perm. of }(1,2,3,4)\text{ in pairs}]\right]$$
$$+\frac{\delta_{a'a}}{m}\left(\frac{\ln s_1}{4\pi}\right)^2\left[\int\frac{d^2p_1d^2p_2}{(2\pi)^4}J(\mathbf{p}_1,\mathbf{p}_2;\mathbf{q}_1\mathbf{q}_2)\frac{-ie^2}{\mathbf{p}_1^2+\mu^2}\frac{-ie^2}{\mathbf{p}_2^2+\mu^2}(2\pi)^2\delta^2(\mathbf{p}_1+\mathbf{p}_2-\mathbf{q}_{12})\int\frac{d^2p_3d^2p_4}{(2\pi)^4}J(\mathbf{p}_3,\mathbf{p}_4;\mathbf{q}_3,\mathbf{q}_4)\right.$$
$$\left.\times\frac{-ie^2}{\mathbf{p}_3^2+\mu^2}\frac{-ie^2}{\mathbf{p}_4^2+\mu^2}(2\pi)^2\delta^2(\mathbf{p}_3+\mathbf{p}_4-\mathbf{q}_{34})+[\text{perm. of }(1,2,3,4)\text{ in two pairs}]\right]+\cdots, \tag{5.13}$$

with

$$\mathbf{q}_{12}=\mathbf{q}_1+\mathbf{q}_2=\mathbf{p}_1+\mathbf{p}_2,\quad \mathbf{q}_{34}=\mathbf{q}_3+\mathbf{q}_4=\mathbf{p}_3+\mathbf{p}_4,$$

where a' and a are the helicities of the electron before and after the scattering. When one puts the two black boxes together, the various parts which correspond to the process shown in Fig. 9 give

$$\tfrac{1}{2}s\frac{1}{4!}\frac{\delta_{a'a}}{m}\frac{\delta_{c'c}}{m}\left[\underset{(a)}{3\left(\frac{\ln s_1}{4\pi}\right)^2}+\underset{(b)}{6\left(\frac{\ln s_1}{4\pi}\right)\left(\frac{\ln s_2}{4\pi}\right)}+\underset{(c)}{3\left(\frac{\ln s_2}{4\pi}\right)^2}\right]$$
$$\times\int\frac{d^2q_1}{(2\pi)^2}\frac{d^2q_2}{(2\pi)^2}\frac{d^2p_1}{(2\pi)^2}\frac{d^2p_2}{(2\pi)^2}J(\mathbf{q}_1,\mathbf{q}_2;\mathbf{p}_1,\mathbf{p}_2)\frac{-ie^2}{\mathbf{q}_1^2+\mu^2}\frac{-ie^2}{\mathbf{q}_2^2+\mu^2}\frac{-ie^2}{\mathbf{p}_1^2+\mu^2}\frac{-ie^2}{\mathbf{p}_2^2+\mu^2}(2\pi)^2\delta^2(\mathbf{q}_1+\mathbf{q}_2-\mathbf{q}_{12})(2\pi)^2\delta^2(\mathbf{p}_1+\mathbf{p}_2-\mathbf{q}_{12})$$
$$\times\int\frac{d^2q_3}{(2\pi)^2}\frac{d^2q_4}{(2\pi)^2}\frac{d^2p_3}{(2\pi)^2}\frac{d^2p_4}{(2\pi)^2}J(\mathbf{q}_3,\mathbf{q}_4;\mathbf{p}_3,\mathbf{p}_4)\frac{-ie^2}{\mathbf{q}_3^2+\mu^2}\frac{-ie^2}{\mathbf{q}_4^2+\mu^2}\frac{-ie^2}{\mathbf{p}_3^2+\mu^2}\frac{-ie^2}{\mathbf{p}_4^2+\mu^2}(2\pi)^2\delta^2(\mathbf{q}_3+\mathbf{q}_4-\mathbf{q}_{34})(2\pi^2)\delta^2(\mathbf{p}_3+\mathbf{p}_4-\mathbf{q}_{34})$$
$$\times\frac{d^2q_{12}}{(2\pi)^2}\frac{d^2q_{34}}{(2\pi)^2}(2\pi)^2\delta^2(\mathbf{q}_{12}+\mathbf{q}_{34}-\mathbf{k}). \tag{5.14}$$

The factors 3 and 6 come from simple counting. It is easy to see that the $\ln s_1$ and $\ln s_2$ factors combine into $3(\ln s/4\pi)^2$, which is frame independent. The two remaining complicated factors are functions of $\mathbf{q}_{12}$ and $\mathbf{q}_{34}$ only, and they are in a convolution form. Hence, the result becomes rather simple in the Fourier space, giving

$$\text{expression (5.14)}=\tfrac{1}{2}s\frac{\delta_{a'a}}{m}\frac{\delta_{c'c}}{m}\int d^2b\,e^{i\mathbf{k}\cdot\mathbf{b}}\frac{1}{2!}[i\chi(\mathbf{s},\mathbf{b})]^2,$$

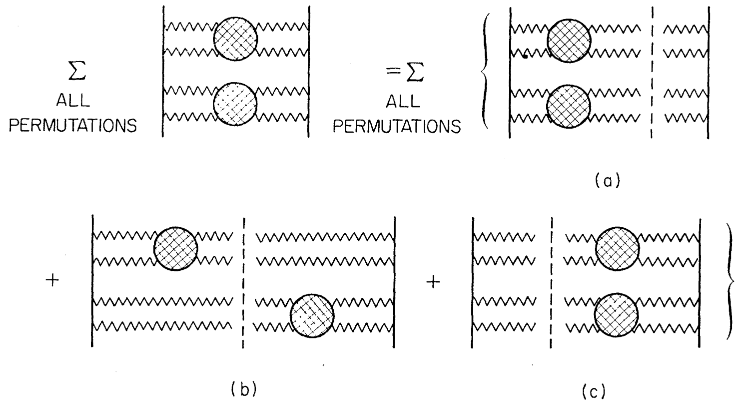

FIG. 9. Same as Fig. 7 with two bubbles iterated in the s channel.

where $\chi(s,b)$ is the Fourier transform of

$$\frac{1}{2}\frac{\ln s}{4\pi}\int\frac{d^2p_1}{(2\pi)^2}\frac{d^2p_2}{(2\pi)^2}\frac{d^2q_1}{(2\pi)^2}\frac{d^2q_2}{(2\pi)^2}J(\mathbf{p},\mathbf{q})\frac{-ie^2}{\mathbf{p}_1{}^2+\mu^2}\frac{-ie^2}{\mathbf{p}_2{}^2+\mu^2}$$
$$\times\frac{-ie^2}{\mathbf{q}_1{}^2+\mu^2}\frac{-ie^2}{\mathbf{q}_2{}^2+\mu^2}(2\pi)^2\delta^2(\mathbf{p}_1+\mathbf{p}_2-\mathbf{k})\times(2\pi)^2\delta^2(\mathbf{q}_1+\mathbf{q}_2-\mathbf{k}).$$

This result agrees with the general eikonal form obtained in III.

VI. COMPARISON AND DISCUSSION

In this paper, we have demonstrated that the asymptotic behavior of QED can be reproduced from an operator droplet model. In particular, we showed that the final expression does *not* depend on the reference frame. If the asymptotic perturbation of QED indeed leads to a correct description for a general scattering amplitude, one might expect that the operator droplet model could supply a useful framework for the description of hadron physics.

We would like to point out the analogy between our model and the parton picture proposed by Feynman.[6] In a parton model, a fast-moving hadron, such as a proton, is described by a group of partons all moving along the direction of the hadron. In general, each of the parton carries a positive fraction x of the total longitudinal momentum. Hadron-hadron scattering can be viewed as the scattering between two groups of partons. Feynman called those partons moving with the first hadron the "right movers," and those moving with the second hadron the "left movers." For final particles, the left and right movers constitute the "fragments" of target and projectile, respectively, as suggested by Benecke, Chou, Yang, and Yen.[1]

The physically interesting part of the scattering amplitude is associated with the interactions between partons of "wee" momentum. A "wee" momentum p_w should satisfy the inequalities $p_{a+}\gg p_{w+}\gg p_{c+}$ and $p_{a-}\ll p_{w-}\ll p_{c-}$; i.e., a "wee" parton carries a momentum whose plus and minus components are much smaller than the large momentum of the incident hadrons. In our language, a "wee" parton lies somewhere in the middle of the available $\ln p_+$ phase space. (In a sense, these "wee" partons are analogous to the particles which are associated with bubbles in the middle, such as evaporation particles.) A "wee" parton cannot be classified unambiguously into one of the incident hadrons. It is confused as to which particle it belongs to. Its sense of motion, i.e., whether it is a left or right mover, depends critically on the reference frame that we are choosing. A reference-frame-independent result can only be obtained after "wee" partons moving in both directions are included. This is precisely what we demonstrated in Sec. V.

The conclusion obtained in Sec. V is also applicable to a theory with both the strong and EM interactions, like the one studied in Sec. III, or to a pure strong-interaction theory with the presence of a neutral vector meson. The black box defined in Sec. III should now include all kinds of strong and EM processes. One can convince oneself from our lower-order calculations that

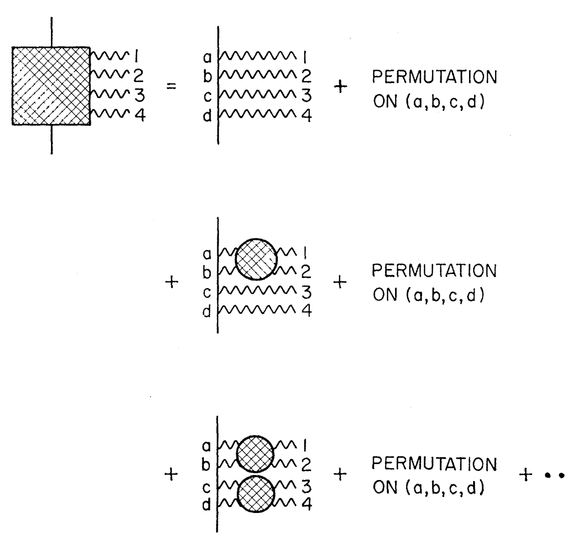

FIG. 10. Relevant partial amplitudes in a black-box expansion for the processes given in Fig. 9.

the order-by-order perturbation result from the operator droplet model reproduces the leading contribution of the amplitude obtained from conventional Feynman diagrams.

One warning should always be kept in mind in summing over these leading diagrams. Although one may show to each finite order of perturbation series that the set of diagrams studied here is composed of leading diagrams at $s=\infty$, it is not clear that the sum of all these diagrams should lead to the correct asymptotic amplitude. It is known that the sum of leading terms sometimes may lead to a completely different result from the exact solution, especially when there is a total cancellation in the leading terms. The Golden rule, that the dominant contributions in any field-theory calculations at $s=\infty$ are given by diagrams with pure vector exchange, is deduced precisely from a study of the leading diagrams. The rule may fail in an exact theory, especially if the coupling of nonvector interactions are strong.

Finally, we wish to emphasize that the main objective of the present investigation is *not* to provide a *quantitative* calculation of the leading $s=\infty$ behavior, but, rather it is to extract certain physical pictures from various class of diagrams. The class of diagrams which are responsible for an operator droplet model is pointed out in Secs. III and V. The relation between these leading diagrams and the operator droplet model may be more fundamental than the present model calculations imply.

ACKNOWLEDGMENTS

The author is indebted to Professor Paul Fishbane for many stimulating discussions and a critical reading of the manuscript, and to Professor Tung-Mow Yan for helpful discussions in related models. The author wishes to thank Professor Sidney Drell and members of the SLAC theory group for their hospitality during the author's visit at SLAC. Finally, he wishes to express his gratitude to Professor R. Torgerson for many critical comments on the presentation of this paper.

APPENDIX: COMMUTATOR RELATIONS ON LIGHT CONE

It was conjectured by Gell-Mann that the equal-time commutator relations between the time components of a vector and another vector (or axial-vector) current satisfy an $SU_3 \times SU_3$ current algebra of the form

$$[\mathfrak{F}_a{}^0(x),\mathfrak{F}_b{}^0(y)]=if_{abc}\mathfrak{F}_c{}^0(x)\delta^3(\mathbf{x}-\mathbf{y})\cdots, \qquad (\mathrm{A1})$$

where f_{abc} is the structure constant of the SU_3 algebra. We would like to show that, under a proper limiting process, Eq. (A1) implies a similar commutator relation for currents on the light cone $x_+=y_+$:

$$[\tfrac{1}{2}\mathfrak{F}_{a+}(x),\tfrac{1}{2}\mathfrak{F}_{b+}(y)]=if_{abc}\tfrac{1}{2}\mathfrak{F}_{c+}(x) \times\delta^2(\mathbf{x}-\mathbf{y})\delta(x_- - y_-). \qquad (\mathrm{A2})$$

On integration over x_- and y_-, we obtain the operator version of the Gell-Mann–Dashen–Fubini sum rule,[16,17]

$$[\sigma_{a+}(\mathbf{x}),\sigma_{b+}(\mathbf{y})]=if_{abc}\sigma_{c+}(\mathbf{x})\delta^2(\mathbf{x}-\mathbf{y}). \qquad (\mathrm{A3})$$

To obtain (A2) from (A1), we make a Lorentz transformation along the third axis:

$$Uj^0(x)U^{-1}=\cosh\lambda\ j^0(x')+\sinh\lambda\ j^3(x') =\tfrac{1}{2}e^{\lambda}j_+(x')+\tfrac{1}{2}e^{-\lambda}j_-(x'),$$

with

$$x_+'=e^{-\lambda}x^3 \quad (x^0=0), \qquad \mathbf{x}_\perp'=\mathbf{x}_\perp, \qquad x_-'=-e^{\lambda}x^3.$$

For fixed x_-' and $e^{\lambda}\to\infty$, we have

$$[\tfrac{1}{2}e^{\lambda}j_+(x_+'=0,\mathbf{x},x_-'),\tfrac{1}{2}e^{\lambda}j_+(y_+'=0,\mathbf{y},y_-')] =\tfrac{1}{2}e^{\lambda}j_+(0,\mathbf{x},x_-')\delta^2(\mathbf{x}-\mathbf{y})\delta(e^{-\lambda}(x_-'-y_-')).$$

Canceling out factors e^{λ}, we get (A2).

As a justification of the limiting procedure, the validity of Eq. (A2) can be checked independently from various free-particle models. With the help of the equations of motion, Eq. (A2) is found to be satisfied for both scalar and Dirac fields.

In the simple case of QED, we know that the charge density operators, the $j^0(x)$'s, commute among themselves at equal time. Hence, the $j_+(x)$'s commute among themselves on the light cone $x_+=$ const. The last relation is precisely what we need to prove Eq. (2.9).

[16] R. Dashen and M. Gell-Mann, Phys. Rev. Letters **17**, 340 (1966); S. Fubini and G. Furlan, Physics **1**, 229 (1964).
[17] K. Bardakci and M. B. Halpern, Phys. Rev. **176**, 1686 (1968).